Synthetic and Systems Biotechnology 7 (2022) 918–927

Contents lists available at ScienceDirect

Synthetic and Systems Biotechnology

journal homepage: www.keaipublishing.com/en/journals/synthetic-and-systems-biotechnology

Engineering *Shewanella carassii,* a newly isolated exoelectrogen from activated sludge, to enhance methyl orange degradation and bioelectricity harvest

Chi Yang [a,b,c,1], Junqi Zhang [a,b,1], Baocai Zhang [a,b], Dingyuan Liu [a,b], Jichao Jia [a,b], Feng Li [a,b,c,**], Hao Song [a,b,c,*]

[a] Frontier Science Center for Synthetic Biology and Key Laboratory of Systems Bioengineering (Ministry of Education), Tianjin University, Tianjin, 300072, China
[b] Collaborative Innovation Center of Chemical Science and Engineering (Tianjin), School of Chemical Engineering and Technology, Tianjin University, Tianjin, 300072, China
[c] Qingdao Institute Ocean Engineering of Tianjin University, Tianjin University, Qingdao, 266200, China

ARTICLE INFO

Keywords:
Microbial fuel cells
WO_3 nanocluster probe
Shewanella carassii
Riboflavin
Methyl orange

ABSTRACT

Electroactive microorganisms (EAMs) play important roles in biogeochemical redox processes and have been of great interest in the fields of energy recovery, waste treatment, and environmental remediation. However, the currently identified EAMs are difficult to be widely used in complex and diverse environments, due to the existence of poor electron transfer capability, weak environmental adaptability, and difficulty with engineering modifications, etc. Therefore, rapid and efficient screening of high performance EAMs from environments is an effective strategy to facilitate applications of microbial fuel cells (MFCs). In this study, to achieve efficient degradation of methyl orange (MO) by MFC and electricity harvest, a more efficient exoelectrogen *Shewanella carassii*-D_5 that belongs to *Shewanella* spp. was first isolated from activated sludge by WO_3 nanocluster probe technique. Physiological properties experiments confirmed that *S. carassii*-D_5 is a Gram-negative strain with rounded colonies and smooth, slightly reddish surface, which could survive in media containing lactate at 30 °C. Moreover, we found that *S. carassii*-D_5 exhibited remarkable MO degradation ability, which could degrade 66% of MO within 72 h, 1.7 times higher than that of *Shewanella oneidensis* MR-1. Electrochemical measurements showed that MFCs inoculated with *S. carassii*-D_5 could generate a maximum power density of 704.6 mW/m^2, which was 5.6 times higher than that of *S. oneidensis* MR-1. Further investigation of the extracellular electron transfer (EET) mechanism found that *S. carassii*-D_5 strain had high level of *c*-type cytochromes and strong biofilm formation ability compared with *S. oneidensis* MR-1, thus facilitating direct EET. Therefore, to enhance indirect electron transfer and MO degradation capacity, a synthetic gene cluster *ribADEHC* encoding riboflavin synthesis pathway from *Bacillus subtilis* was heterologously expressed in *S. carassii*-D_5, increasing riboflavin yield from 1.9 to 9.0 mg/g DCW with 1286.3 mW/m^2 power density output in lactate fed-MFCs. Furthermore, results showed that the high EET rate endowed a faster degradation efficient of MO from 66% to 86% with a maximum power density of 192.3 mW/m^2, which was 1.3 and 1.6 times higher than that of *S. carassii*-D_5, respectively. Our research suggests that screening and engineering high-efficient EAMs from sludge is a feasible strategy in treating organic pollutants.

Peer review under responsibility of KeAi Communications Co., Ltd.
* Corresponding author. Frontier Science Center for Synthetic Biology and Key Laboratory of Systems Bioengineering (Ministry of Education), Tianjin University, Tianjin, 300072, China.
** Corresponding author. Frontier Science Center for Synthetic Biology and Key Laboratory of Systems Bioengineering (Ministry of Education), Tianjin University, Tianjin, 300072, China.
E-mail addresses: messilifeng@163.com (F. Li), hsong@tju.edu.cn (H. Song).
[1] Equal contribution.

https://doi.org/10.1016/j.synbio.2022.04.010
Received 16 March 2022; Received in revised form 26 April 2022; Accepted 27 April 2022
Available online 1 May 2022

1. Introduction

Environmental pollution and energy crisis have become serious challenges for global sustainable development. Domestic, industrial, and farming wastewaters are essential categories of environmental pollutants that contain enormous amount of chemical energy stored in organics [1]. Nevertheless, these energies are often largely lost or dissipated in the actual treatment process. Recovering potential energy meanwhile treating wastewater by cost-effective technologies can contribute to relieving energy shortage and environmental pollution issues [2]. Microbial fuel cells (MFCs) have attracted widespread attention for their dual function of energy recovery and wastewater treatment by conversion of chemical energy from partial carbohydrates and organic acids in wastewater into electrical energy by biocatalysts [1,3–6]. Notably, the physiological characteristics and electron transfer ability of electroactive microorganisms (EAMs) as biocatalysts in MFCs directly affect the catalysis performance [7].

Generally, EAMs have been isolated and obtained mainly from *Geobacter*, *Shewanella*, *Pseudomonas*, and *Rhodoferax* sp [7]. Among these strains, the extracellular electron transfer (EET) mechanism and synthetic biology modification strategies based on *S. oneidensis* MR-1 and *G. sulfurreducens* are extensively studied [8,9]. Both strains have multiple EET mechanisms, including direct EET mediated by *c*-type cytochromes [10–12] and conductive nanowires [13–16], and indirect electron transfer mediated by electron mediators [17–19]. However, the low electron transfer capacity of these EAMs limits the potential applications in wastewater treatment and energy recovery [20,21]. Therefore, to overcome this issue, numerous studies have been conducted by researchers from broadening substrate utilization, improving electron generation, and enhancing extracellular electron transfer [22–24]. Although these synthetic biology strategies could facilitate electron production and efficient transfer at a certain level, a higher threshold of extracellular electron transfer capacity is still not achieved due to their physiological properties and the different of EET mechanisms. Thus, there is an urgent need to isolate and screen novel EAMs with superior physiological characteristics and electron generation capacity.

Activated sludge contains a diverse range of microorganisms, of which EAMs are one of the most important categories, actively involved in the degradation and resourceful conversion of wastewater pollutants [25,26]. In order to improve wastewater treatment and resource utilization, researchers have developed various methods for enrichment and screening of EAMs using activated sludge as an inoculum source in recent years, including MFC electrode enrichment, WO_3 nanoprobe coloration [27–30], peroxidase coloration [31–33], and dye reduction [34–36]. However, most of the microorganisms isolated and selected from activated sludge mainly were exoelectrogens with low electron transfer efficiency, which cannot realize efficient degradation and power recovery of organic wastewater containing azo dyes [37,38] and domestic wastewater [5,39].

Here, to realize efficient degradation of methyl orange (MO) meanwhile harvest clean electricity, a highly electroactive strain *S. carassii*-D_5 was isolated from activated sludge. The physiological analysis confirmed that *S. carassii*-D_5 was a Gram-negative strain which could maintain survival and power production using lactate as carbon source and electron donor. We further measured the electrochemical characterization of *S. carassii*-D_5, which showed that the maximum power density was 704.6 mW/m^2. The extracellular electron transfer mechanism of *S. carassii*-D_5 was probed by using electrochemical and spectroscopic methods, demonstrating that *S. carassii*-D_5 mostly conducted extracellular electron transfer via a direct electron transfer channel mediated by cytochromes and electroactive biofilms. In addition, to further enhance its extracellular electron transfer and MO degradation capacity, a riboflavin synthesis gene cluster *ribADEHC* from *Bacillus subtilis* was heterologously expressed in *S. carassii*-D_5, increasing riboflavin yield from 1.9 to 9.0 mg/g DCW with 1286.3 mW/m^2 power density output in lactate fed-MFCs. Furthermore, the strengthen extracellular electron transfer capacity resulted in an increase in the first order rate constants (k) of the MO degradation level from 0.0175 h^{-1} to 0.0316 h^{-1} with a maximum power density of 192.3 mW/m^2 in MFC.

2. Materials and methods

2.1. MFC setup

Activated sludge from Tianjin Guozhong Runyuan Sewage Treatment Co., Ltd (Tianjin, China) was used as inoculum for enrichment in dual-chamber MFCs. For the dual-chamber, each chamber had a volume of 140 mL and they were separated by a Nafion 117 membrane (DuPont Inc., USA). The carbon cloth pretreated with hydrochloric acid (1 M) and acetone solution was employed as working electrodes for anode (2.5 cm × 3.0 cm) and cathode (2.5 cm × 3.0 cm). After simple precipitation treatment, 120 mL activated sludge was inoculated in the anode for enrichment. The cathode was filled with an equal volume of electrolyte solution (50 mM K_3 [$Fe(CN)_6$], 50 mM KH_2PO_4, and 50 mM K_2HPO_4) as electron acceptors. For the external circuit of the MFCs, copper wires were used as a conductor to connect electrodes and external resistance (2 KΩ) and the output voltage was recorded by a digital multimeter (DT9205A) [40,41]. Next, the activated sludge-MFC was run continuously at room temperature and we replaced the anolyte and catholyte with new activated sludge and electrolyte solution when the output voltage dropped lower than 100 mV.

2.2. Bacterial isolation, identification, and preservation

After repeated inoculation for 2–3 times, removed the anode chamber carbon cloth when the output voltage was stable to screen and identify EAMs. The specific steps of the screening method were as following: the anode carbon cloth was serially diluted in phosphate buffer solution (PBS, 50 mM, pH = 7.0) with the series of 10^{-1} to 10^{-9} to form bacterial suspension, which were inoculated on plates containing the Luria-Bertani (LB) agar at 37 °C. After 48 h of incubation and enrichment period, these pure bacteria colonies with different appearance and morphology were streaked on the LB agar plate. When many single colonies grew on the plate, the slightly cooled LB agar containing WO_3 nanoparticles was poured on it and then cultured in an incubator [42]. Subsequently, the blue areas as-obtained in the plate were used as inoculation sources for further screening of EAMs and the EAMs were then purified by streaking of the colonies repeatedly on nutrient agar at least 5 times until single colonies were obtained. In the meantime, the colonies with obvious differences in characteristics like morphology, color, size, surface, and edge were selected and inoculated in LB broth for overnight culture, and the determination of cell density (optical density at 600 nm, OD_{600}) was adjusted with PBS (OD_{600} = 0.5, 50 mM, pH = 7.0). Then, 100 μL bacterial solution and nano-WO_3 solution were added to the 96-well cell culture plate, respectively, and finally the paraffin oil was added to isolate oxygen. The 96-well plate was cultured in 30 °C incubator, and *S. oneidensis* MR-1 [43] was used as a positive control to observe the color change in time. The printer was used to scan the images, and compared the speed and depth of the color changes in pictures, so as to screen out the EAM with strong bioelectricity generation capacity. Pure cultures of strains were stored routinely at −80 °C in LB broth supplemented with 50% (v/v) glycerol. For phylogenetic analysis, the sequences were aligned using MEGA version 7.0 with reference sequences of *Shewanella* species available in the NCBI GenBank (National Center of Biotechnology Information) database by BLAST search, and the branching stability of the tree was analyzed by Bootstrap, repeated 1000 times. The genetic relationship of the isolated strain with high bioelectricity generation capacity was compared as the previous reports by the construction of phylogenetic tree based on the results of a neighbor-joining analysis of 16S rRNA sequences which was amplified by Polymerase Chain Reaction (PCR) with the universal primers 27F (5′ - AGAGTTTGATCCTGGCTCAG-3′) and 1492R (5′ -

GGTTACCTTGTTACGACTT - 3′) [44] for the strain.

2.3. Bacteria physiological and biochemical characterization

The isolated strain was cultured in LB broth at 30 °C for 12 h, then15-20 μL liquid samples were evenly spread on 2.0 cm × 3.0 cm microscopy slides, dried at room temperature, and the samples were then heat fixated (1s on open flame, repeated 3 times) while simultaneously Gram stained by hand [45]. Its cellular morphology on LB agar plate was observed by using a camera (smart series RZSP-200C). To determine condition of cell growth, M9 medium containing different carbon sources, including acetate, lactate, glycerol, fructose, sucrose, xylose, galactose, and glucose was configured, the added concentrations of each carbon source were 5 mM, 10 mM, 15 mM, and 20 mM, respectively, and the optimal substrate growth conditions were evaluated by OD_{600}. 200 μL bacterial culture suspension was inoculated into 96-well plate, incubating at 30 °C for 200 rpm, and samples were withdrawn periodically for the determination of cell density, and the OD_{600} value was measured by ultraviolet and visible spectrophotometer (TU-1810, Beijing Purkinje General Instrument Co. Ltd., China) to obtain the growth situation of the strain. In addition, we further determined the contact angle (CA, θ W) and the affinity of the cells for n-hexadecane. The contact angle was measured by a CA goniometer, SPCA-X3 series (HARKE, Shanghai, China).

2.4. Electrochemical analyses

The bacterial culture suspension grown overnight was transferred to the LB broth at a ratio of 1:100. After growing for approximately 12 h at 30 °C for 200 rpm, the concentration of the cell suspension was adjusted to OD_{600} = 1.0 and inoculated into the anode chamber of MFCs, including M9 buffer, 5% LB broth, and 20 mM lactate. Three groups were set in parallel, and the difference to the activated sludge-MFC was that the size of carbon cloth electrode used in the anode chamber was 1.0 cm × 1.0 cm. Meanwhile, MFCs inoculated with *S. oneidensis* MR-1 were constructed by the same method as a control experiment. When the voltage of MFCs reached the peak and remained the steady state, removing the resistor, standing for 30 min, and using electrochemical workstation (CH Instrument, Shanghai, China) to test the performance of the MFC by Cyclic voltammetry (CV) and Linear sweep voltammetry (LSV) at room temperature. The CV curves were obtained by testing the MFC on a three-electrode configuration with a scan rate of 1.0 mV/s when the Ag/AgCl (KCl saturated) reference electrode was added to the anode, and the initial potential of the scan was set at −0.7 V. The LSV and polarization curves analysis was conducted on a two-electrode mode, and the initial potential was set to −0.87 to −0.1 V with a slow scanning rate of 0.1 mV/s [40]. The internal resistance (R_{int}) of MFC was calculated using the following Eq. (1):

$$R_{int} = \Delta E / \Delta I \quad (1)$$

Here, ΔE (V) represents the voltage output change value of MFCs, and ΔI (I) represents the current output change value of MFCs.

2.5. Construction of engineered strains

The sequences of *ribADEHC* genes coding the riboflavin synthesis pathway from *B. subtilis* were identified and extracted from KEGG (http://www.kegg.jp/kegg/genes.html). Then each coding sequence was optimized by JCAT (http://www.jcat.de/) and the plasmid pYYDT-*ribADEHC* (pYYDT-C_5) combined with an isopropyl β-D-1-thiogalactopyranoside (IPTG)-inducible promoter P*tac* which can drive the expression of riboflavin synthesis pathway encoding genes was constructed through BioBrick™ assembly method in *E. coli* WM3064 [46]. The plasmid pYYDT-C_5 was then transformed into the isolated strain by conjugation and 0.059 g/L 2, 6-diaminopimelic acid (DAP) was added for the growth of *E. coli* WM3064 [40]. Whenever needed, 50 μg/mL kanamycin (kana) was added.

2.6. Riboflavin, cytochromes and MO measurements

The riboflavin in the LB fermentation broth was analyzed by high-performance liquid chromatography (HPLC) at a wavelength of 270 nm. All standard solutions and samples supernatants were filtered and assayed by eluting with methanol-water (50: 50, v: v) of flow remained 0.6 mL/min for 25 min on a poroshell column system (C18 column, 5 μm, 4.6 × 250, Shim-pack GIST) at 35 °C. In the meantime, the cells harvested by centrifugation at 12,000 rpm for 15 min were resuspended and washed twice with PBS buffer, then the resulting pellets were dried at 105 °C to weigh the dry cell weight (DCW) or scanned at full wavelength (from to 300–600 nm) in a transparent 96-well plate after ultrasonication (200 W, ultrasonic for 2 s, pause for 1 s, a total of 1 min) to measure all the amount of *c*-type cytochromes inside and outside of the cells.

To enable the degradation of MO meanwhile generating electrical energy, we constructed a new MFC in which the anode solution was composed of M9 medium inoculated with *S. carassii*-D_5 strain and the cathode was composed of MO solution. The anode electrolyte solution of MFCs included M9 buffer, 5% LB broth, 20 mM lactate as before. The cell density of *S. carassii*-D_5 was adjusted to $OD_{600} = 0.4$ and then dispersed it into the MFC anode. The cathode electrolyte solution was replaced with MO at a concentration of 50 mg/L, pH = 3 [47] as electron acceptors. The buffer solution was prepared by dissolving 6.8 g KH_2PO_4 in 900 mL distilled water and adjusting pH = 3 with dilute phosphoric acid. Moreover, the anaerobic cathode chamber was purged with high purity nitrogen for at least 20 min before running. During the operation, the MFCs were sampled at 0 h, 12 h, 24 h, 36 h, 48 h, 60 h, and 72 h to detect MO concentration. 2 mL MO solution was taken from the MFC cathode chamber, diluted and scanned by ultraviolet and visible spectrophotometer (TU-1810, Beijing Purkinje General Instrument Co. Ltd., China) to determine the MO concentration [47]. Then the decolorization rate *R* of MO was calculated using the following Eq. (2):

$$R = (A_0 - A_t) / A_0 * 100\% \quad (2)$$

In this case, A_0 represents the initial absorbance value of the MO solution, and A_t represents the reaction absorbance value of the MO solution.

The linear relationship of $ln\ (C_t/C_0)$ vs t shows that MO reduction follows pseudo-first-order kinetics.

$$ln\ (C_t / C_0) = - kt \quad (3)$$

where C_0 is the initial MO concentration (mg/L), C_t is the MO concentration at time t (mg/L), and t is the reaction time (s). Therefore, the kinetics constant k can be obtained through regression using Eq. (3) [47].

2.7. Characterization of the anode biomass

The anodic carbon cloth covered with biofilm was taken out and placed in a tube containing 10 mL PBS buffer, vortexing for 2 min to obtain uniform bacterial suspension, then the diluted solution was coated on the LB agar plate. After incubation at 30 °C for 24 h, colony forming units (CFU) were counted [40]. Meanwhile, the uniform bacterial suspension containing the electrode-attached cells was centrifuged at 15,000 rmp for 5 min and the resulting pellets were mixed with B-PERII bacterial protein extraction reagent (Thermo Fisher Scientific. Walthman, MA, USA) to solubilize the proteins according to the manufacturer's instructions, then the Bicinchoninic acid (BCA) protein assay kit was used to determine the biomass content of anode surface [41,48]. Three biological replicates were performed under each of the above experimental conditions.

3. Results and discussion

3.1. Bacterial enrichment, isolation, and identification

In this study, for the purpose of enriching and isolating highly electroactive microorganisms, the MFCs were constructed using activated sludge from wastewater treatment plants as anolyte as well as microbial community in the sludge as anode microorganisms. The voltage output performance of activated sludge-MFCs was investigated (Fig. S1). It was obvious that the activated sludge-MFC could maintain a maximum output of 242.3 ± 12 mV over three generation cycles, which indicated that a stable microbial community was formed at the electrode to release electrons. After 250 h of enrichment, anode carbon cloth containing electroactive bacteria was resuspended in PBS buffer, and then incubated with 10^{-9} CFU/mL concentration on LB agar plates by combining WO_3 nanomaterials as probes for rapidly identifying EAMs [28]. Based on WO_3 electrochromic, we obtained an electroactive strain with strong electrochromic ability (Fig. S2).

To further identify the properties of the isolated electroactive strain, the 16S rRNA fragment was amplified by PCR with universal primers 27F/1492R. Based on the results of the 16S rRNA gene sequencing (**Seq. S1**), we successfully constructed a phylogenetic tree of the strain using the neighbor-joining method and identified that the strain belonged to the genus *Shewanella carassii*, with 99.79% sequence similarity to *Shewanella carassii* strain LZ2016-166 (GenBank accession number MF164483.1) in Fig. 1. We thus named it as *Shewanella carassii*-D_5. The information on the other isolated strains was provided in Table S1.

3.2. Biological characterization of the Shewanella carassii-D_5 strain

To characterize the morphological properties of *Shewanella carassii*-D_5 strain, we first observed its cellular morphology on LB agar plate using a smart camera. As shown in Fig. 2A, the colonies were round or elliptical with neat edges and opaque pink-orange color. The Gram stain results indicated that *S. carassii*-D_5 was Gram-negative (Fig. S3) with a short rod-like morphology, similar to *S. oneidensis* MR-1 [49]. Scanning electron microscopy (SEM) and transmission electron microscope (TEM) were further used to observe cell ultrastructure (Fig. 2B–C). It was found that *S. carassii*-D_5 was rod-shaped strain with a size of 2.0–3.0 μm and a rough cell surface containing extracellular polymeric substances (EPS), which may contribute to biofilms formation to promote energy conversion and protect them against adverse environmental influences [50].

In addition, to determine the optimal carbon source for the growth of *S. carassii*-D_5, the cell growth was monitored by adding different concentration gradients (5–20 mM) acetate, lactate, glycerol, fructose, sucrose, xylose, galactose, and glucose to the M9 medium as sole carbon sources, respectively. As shown in Fig. 2D, the results indicated that *S. carassii*-D_5 enabled metabolizing lactate and acetate but cannot utilize other carbon sources. In particular, cell growth was enhanced with

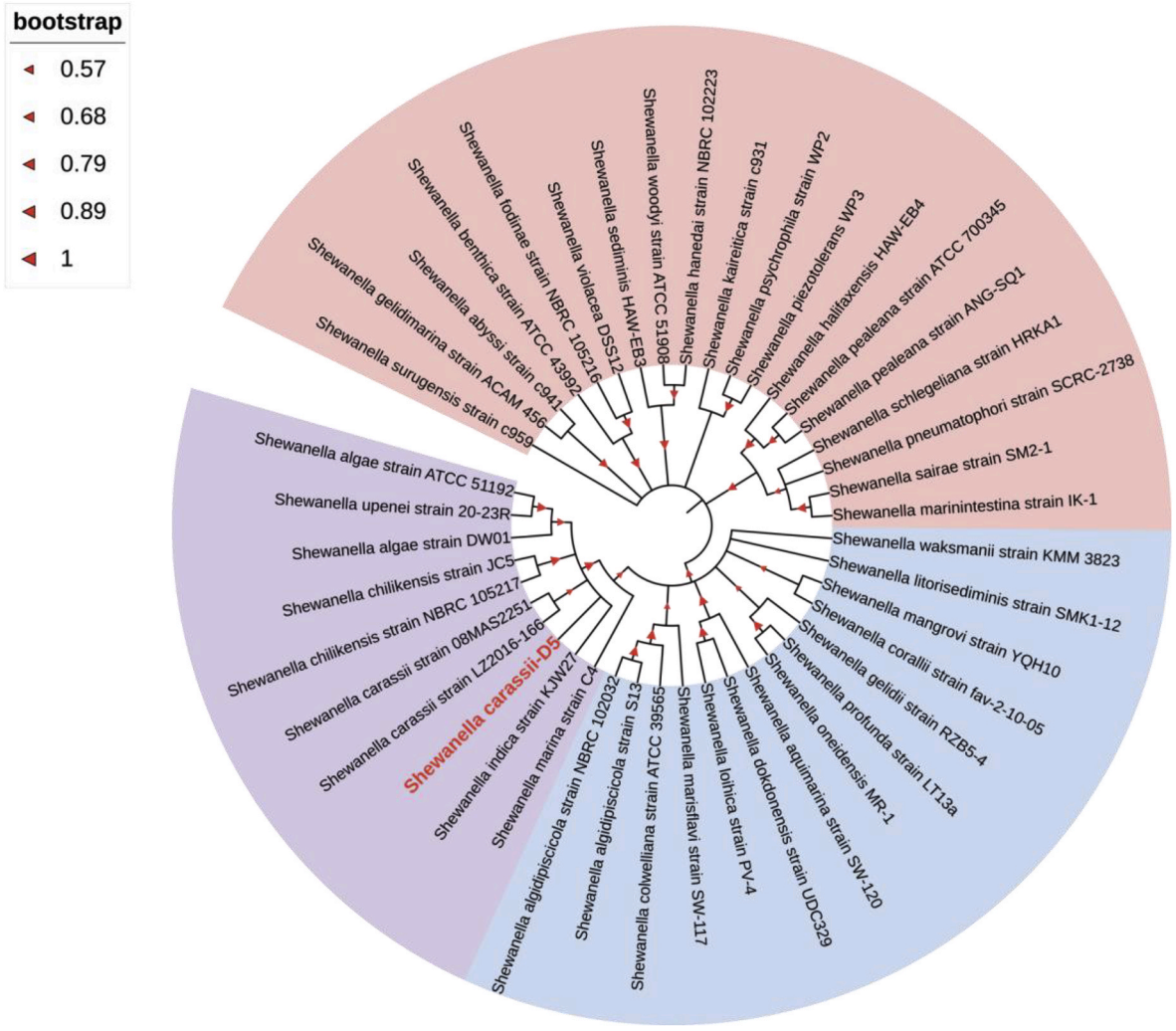

Fig. 1. Phylogenetic tree based on the results of a neighbor-joining analysis of 16S rRNA sequences for the strain *Shewanella carassii*-D_5 and various members of *Shewanella* spp. Numbers at nodes indicate bootstrap values > 50% (expressed as percentages of 1000 replications).

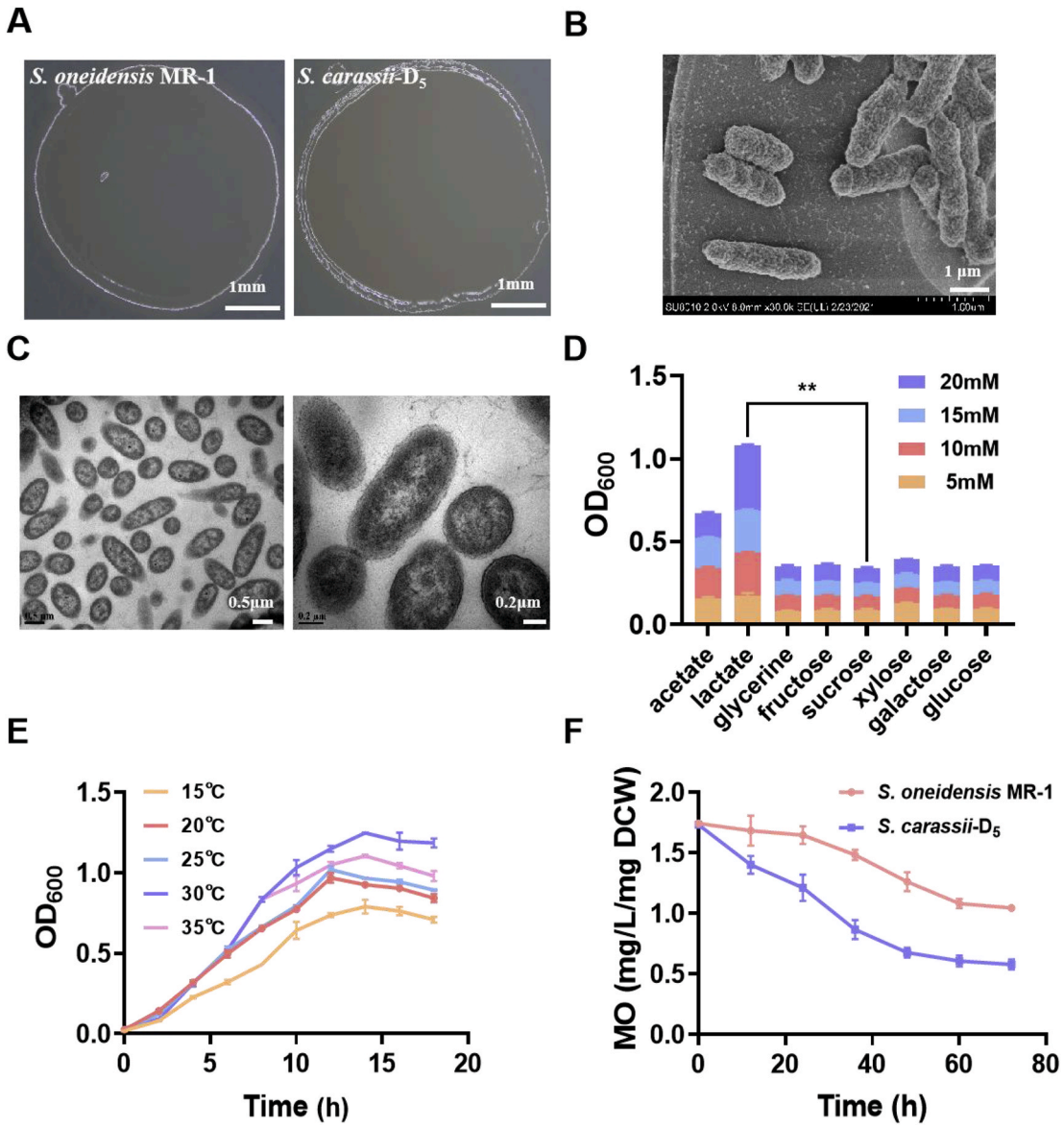

Fig. 2. Characterization of biological properties of *S. carassii*-D_5. (A) Colony morphology photo of the bacteria inoculated on LB agar plate. (B) SEM characterization of the isolated strain. (C) TEM characterization of the bacteria. (D) OD_{600} of inoculated with the bacteria adding acetate, lactate, glycerol, fructose, sucrose, xylose, galactose, and glucose as substrates at concentration ranging from 5 to 20 mM. (E) Optimization of optimum growth temperature of *S. carassii*-D_5 with 20 mM lactate as the sole carbon source. (F) Comparison of MO degradation ability between *S. carassii*-D_5 and *S. oneidensis* MR-1. Three biological replicates were performed. (**: $p < 0.01$; *: $p < 0.05$).

increasing of lactate concentration, which is the same as the profiles of *Shewanella*. To investigate the optimum culture temperature of *S. carassii*-D_5, we further determined its growth activity at different temperatures using 20 mM lactate as the carbon source. As revealed in Fig. 2E, the optimum culture temperature of *S. carassii*-D_5 was 30 °C, which is consistent with *S. oneidensis* MR-1. However, the growth of *S. carassii*-D_5 strain is relatively weaker than *S. oneidensis* MR-1 (Fig. S4).

The UV–Vis spectra of MO solution in cathode of MFCs inculcated with the wide type *S. carassii*-D_5 under illumination at different reaction times was seen in Fig. S5 that the *S. carassii*-D_5 achieved the degradation of the MO solution. The MO removal rate of *S. carassii*-D_5 was shown in Fig. 2F, which showed a more rapid MO removal process compared to *S. oneidensis* MR-1. Especially, within 72 h, *S. carassii*-D_5 could degrade about 66% of MO, which was about 1.7 times higher than that of *S. oneidensis* MR-1 (40%), indicating that the superior MO degradation ability was mainly caused by the high EET of *S. carassii*-D_5 rather than the cell growth.

3.3. Electrochemical characterization of *S. carassii-D5*

The power density and the polarization curve are important indicators to assess the bioelectricity generation performance of MFCs. Here, to evaluate the specific power production capacity of *S. carassii*-D_5, we systematically measured the above indicators in MFCs. As shown in Fig. 3A, the power density output curves shown that *S. carassii*-D_5 strain obtained a maximum power density of 704.6 mW/m^2, which was increased by 5.6 times compared with that of the *S. oneidensis* MR-1 (125.0 mW/m^2). The polarization curve reflected the relationship between the potential and the current when the external resistance was reduced. The dropping slope in the polarization curve of *S. carassii*-D_5 was smaller (R_{int} = 1670.0 Ω), indicating the smaller internal resistance of MFC comparing with *S. oneidensis* MR-1 (R_{int} = 5317.0 Ω). The corresponding output voltage was shown in Fig. S6. Moreover, the redox reaction kinetics at cell-electrode interfaces was further conducted by CV [19,51]. In Fig. 3B, *S. carassii*-D_5 and *S. oneidensis* MR-1 exhibited an

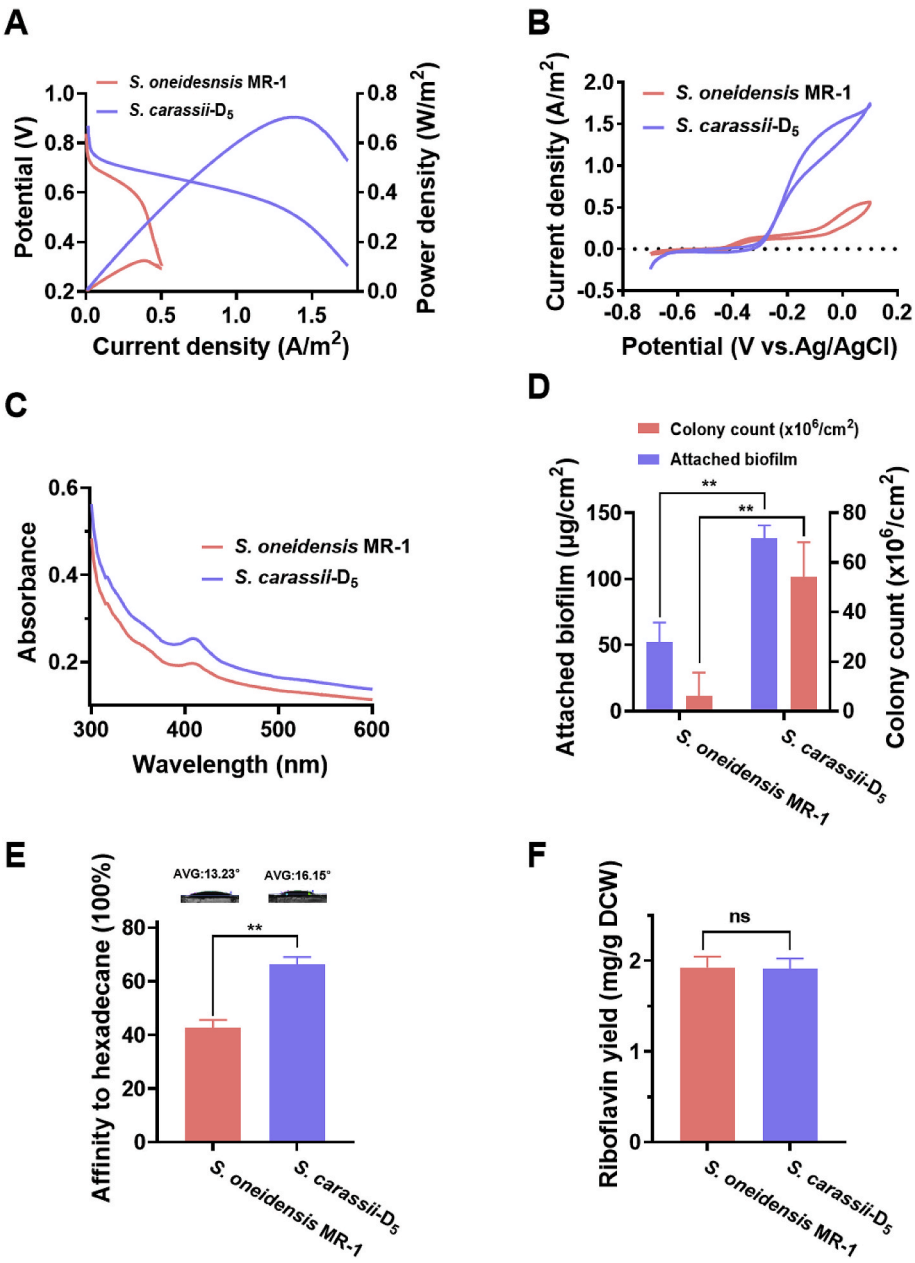

Fig. 3. Electrochemical characterization of *S. carassii*-D_5. (A) LSV and the polarization curves and (B) CV curves of *S. carassii*-D_5 (OD_{600} = 1.0) inoculated in MFCs with lactate as electron donor. (C) Cytochrome level measurement in the LB fermentation broth at OD_{600} = 1.0. (D) The attached biofilm and colony count on anode carbon cloth in MFCs with lactate as electron donor. (E) Water contact angle observation and the affinity of the cells for n-hexadecane. (F) Riboflavin production in the LB fermentation broth at OD_{600} = 1.0. Three biological replicates were performed. (**: $p < 0.01$; *: $p < 0.05$; ns: no significance; $p > 0.05$).

obvious riboflavin redox peak originating from ~ −0.4 V (vs. Ag/AgCl). Notably, the redox peak of *S. carassii*-D_5 was slightly lower than that of *S. oneidensis* MR-1. In the meantime, we also found a redox peak on the CV curve starting from ~ −0.3 V, which corresponded to OM *c*-Cyts, thus speculated that outer membrane cytochromes main played a major role in extracellular electron transfer in *S. carassii*-D_5 strain.

Numerous studies demonstrated that the mechanism of EET between EAMs and electrodes is conducted mainly by direct transfer mediated by *c*-type cytochromes or conductive nanowires and indirect transfer mediated by electron mediators [9]. Therefore, to reveal the EET mechanism of *S. carassii*-D_5, we further measured the cytochromes, adhesion biomass and riboflavin in MFC which were regarded as playing important roles in EET process of *Shewanella*. A full wavelength scan results showed that *S. carassii*-D_5 had a higher density of cytochromes expression than that of *S. oneidensis* MR-1, suggesting that *S. carassii*-D_5 could depend on abundant cytochromes directly involving in extracellular electron transfer (Fig. 3C). The DCW of the anode chamber and biofilm loading on anodic carbon cloth was determined. As shown in Fig. 3D, *S. carassii*-D_5 had a relatively high biomass (131.0 ± 9.6 μg/cm^2) on the anode surface, ~2.5-fold higher than *S. oneidensis* MR-1 (52.3 ± 14.9 μg/cm^2). Meanwhile, the cell count results also showed that there were massive *S. carassii*-D_5 cells attached on the anode carbon cloth (58.2 ± 12.0 × 10^7/cm^2), which was consistent with the SEM results (Fig. S7). However, there was no significant difference in the total biomass in the anode chamber, which indicated a significant advantage in biofilm formation of *S. carassii*-D_5 over *S. oneidensis* MR-1. In addition, it is well know that bacterial attachment to a surface is the initial step in biofilm formation and hydrophilicity might be the dominant factor affecting bacterial adhesion, and strains with relatively strong hydrophobicity are more likely to aggregate to form biofilms [52]. To elucidate the mechanism of high loading of the anodic biofilm, we further determined the contact angle (θ W), as well illustrated in Fig. 3E, the contact angle of *S. carassii*-D_5 was 16.15°, while that of *S. oneidensis* MR-1 was 13.23°. Normal hexadecane-grown cells showed strong capacity in adhering to the hydrocarbon-water interface [53]. Here, it was further shown that the hydrocarbon adhesion rate of *S.*

carassii-D_5 was 66.3%, which was ~1.5 times higher of *S. oneidensis* MR-1 (42.6%). In brief, the cell surface hydrophobicity of *S. carassii*-D_5 was higher than that of *S. oneidensis* MR-1, the abundant EPS of cells which was strengthened contact interaction between cells and electrode surface, thus enhancing the cell coverage on electrode. Besides, we further determined the amount of riboflavin synthesized in *S. carassii*-D_5 (Fig. 3F). It was found that *S. carassii*-D_5 could produce a riboflavin level of 1.9 mg/g DCW, similar to *S. oneidensis* MR-1, which further supported the previous speculation that direct EET mechanism played an essential role.

3.4. Enhanced indirect electron transfer by expressing riboflavin synthesis pathway in *S. carassii*-D_5

Recent studies have found that enhancing the extracellular electron transfer rate not only enhances power output but also promotes MO degradation [19,54,55]. Therefore, to further boost extracellular electron transfer and MO downgrade, an available inducible promoter P_{tac} and the riboflavin biosynthetic gene cluster *ribADEHC* from *B. subtili* were assembled into *S. carassii*-D_5 to construct recombinant strain *S. carassii*-D_5-C_5 (Fig. 4A). Subsequently, the inducible plasmid expression level was further optimized by measuring cell density. As shown in Fig. 4B, the optimum concentrations of IPTG and kana obtained after

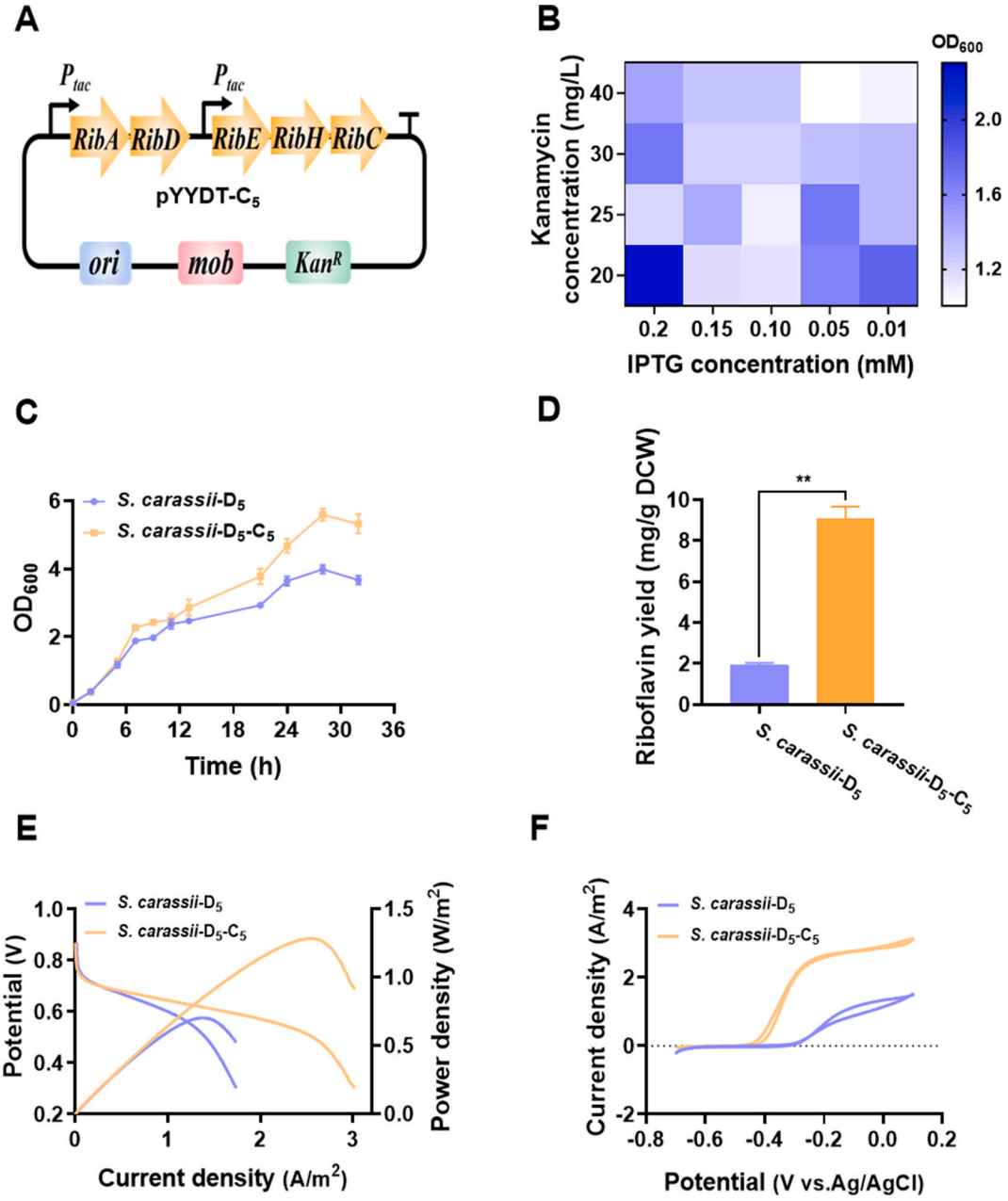

Fig. 4. Enhanced production of riboflavin by engineering *S. carassii*-D_5 *via* synthetic biology approach. (A) Schematic plasmid map of P_{tac} promoter combined with *RibA, RibD, RibE, RibH,* and *RibC* genes expressing vectors. The plasmid was assembled into *S. carassii*-D_5 to construct recombinant strain *S. carassii*-D_5-C_5 for the enhanced riboflavin metabolism. (B) The appropriate concentrations of IPTG and kana for growth metabolism of engineered strain. (C) Growth curves of the *S. carassii*-D_5-C_5 and *S. carassii*-D_5 in LB fermentation broth with final optimal concentration of 0.2 mM IPTG and 20 mg/L kana at 30 °C for 32 h. (D) Concentration of riboflavin produced by recombinant strain *S. carassii*-D_5-C_5 and the control strain *S. carassii*-D_5 in the broth. (E) LSV and the polarization curves and (F) CV curves of recombinant strain *S. carassii*-D_5-C_5 and the control strain *S. carassii*-D_5 (OD_{600} = 1.0) inoculated in MFCs with lactate as electron donor. Three biological replicates were performed. (**: $p < 0.01$; *: $p < 0.05$).

optimization were 0.2 mM and 20 mg/L, respectively. Fig. 4C showed that overexpressing the riboflavin synthesis pathway in *S. carassii*-D_5 exhibited a superior growth under aerobic conditions, indicating that riboflavin synthesis promoted cellular metabolic activity. As shown in Fig. 4D, the riboflavin yield secreted by the engineered strain was ~9.0 mg/g DCW, which was 4.7-fold higher than that of the control strain (1.9 mg/g DCW). To evaluate the electricity generation capacity of using lactate, *S. carassii*-D_5-C_5 was further inoculated to lactate-fed MFC. The output voltage results showed that the electron output capacity of *S. carassii*-D_5-C_5 was significantly higher than that of *S. carassii*-D_5 (Fig. S8). In Fig. 4E, the maximum power density of recombinant strain *S. carassii*-D_5-C_5 was 1286.3 mW/m^2, ~1.8 times than that of *S. carassii*-D_5 (704.6 mW/m^2). The slope of the polarization curve of *S. carassii*-D_5-C_5 was smaller than that of *S. carassii*-D_5, which indicated that the MFC inoculated with *S. carassii*-D_5-C_5 strain (R_{int} = 803.0 Ω) had a lower internal resistance compared to *S. carassii*-D_5 (R_{int} = 1670.0 Ω). Moreover, the redox reaction kinetics at cell-electrode interfaces was conducted by CV in Fig. 4F. Compared to *S. carassii*-D_5, it is obviously that the *S. carassii*-D_5-C_5 exhibited a higher riboflavin redox peak originating from ~ −0.4 V (vs. Ag/AgCl), which indicated that the riboflavin-mediated EET was strengthened. Meanwhile, a higher OM *c*-Cyts redox peak on the CV curve starting from ~ −0.3 V was found, which indicated more riboflavin can bound with cytochromes to form semi-quinones, accelerating the extracellular electron transfer by "single-electron redox reaction" [56]. In conclusion, all these results suggested that the presence of a relatively higher level of riboflavin synthesized by integrating riboflavin synthesis module could increase the bioelectricity generation and extracellular electron transfer capacity.

3.5. MO degradation with simultaneous power generation by engineered *S. carassii*

The MO removal capacity of MFC makes it a sustainable technology

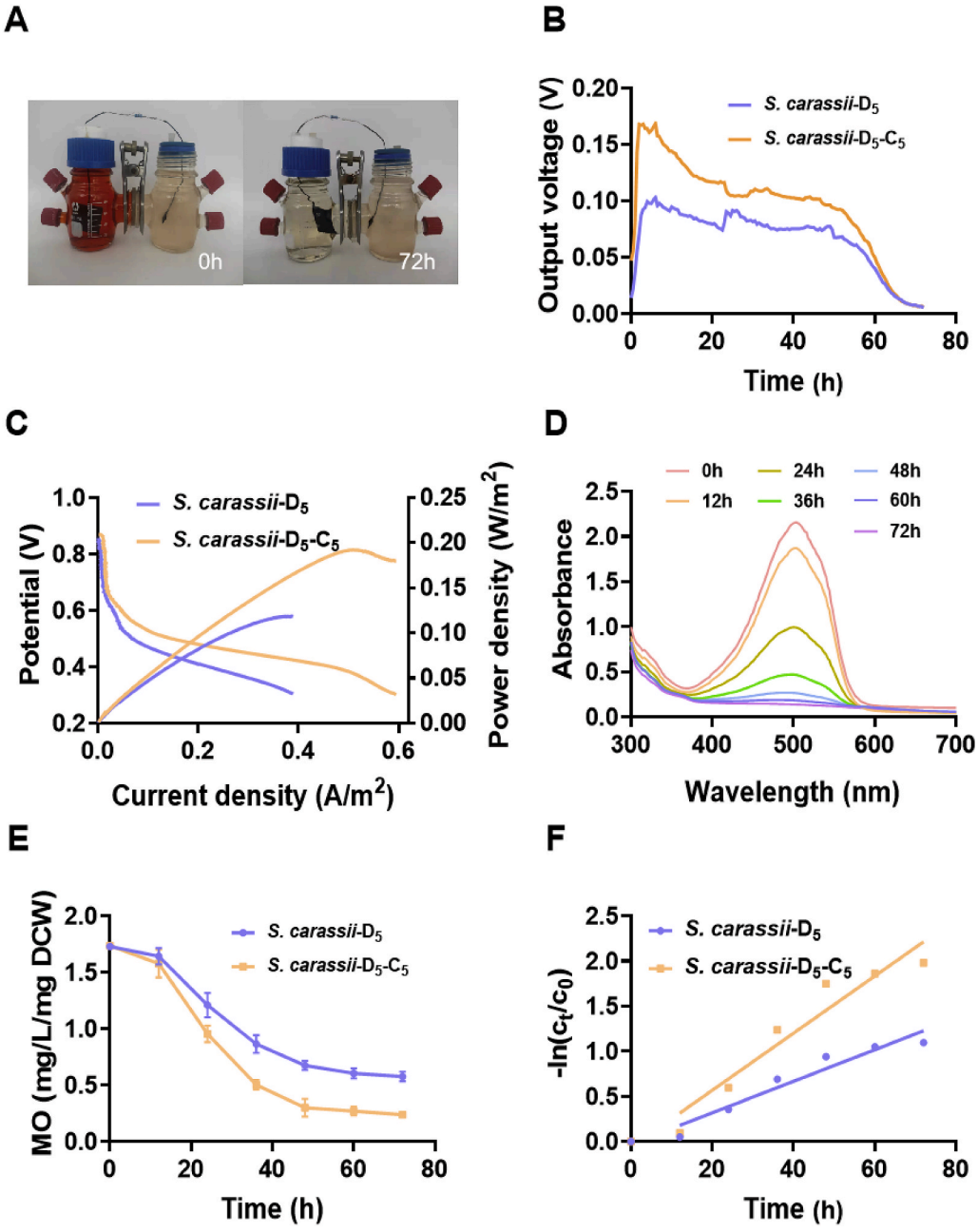

Fig. 5. MO reduction by the recombinant strain *S. carassii*-D_5-C_5 and *S. carassii*-D_5. (A) Structural design of MFC for simultaneous MO decolorization and bioelectricity generation. (B) Voltage output obtained from the MFCs operated for one discharge cycle using MO solution as electron acceptor in cathode (pH = 3, initial MO concentration was 50 mg/L). (C) LSV and the polarization curves of the MFCs. (D) The UV–Vis spectra of MO solution in cathode of MFCs inculcated with the recombinant strain *S. carassii*-D_5-C_5 under illumination at different reaction times. (E) Characterization of MO degradability in cathode. (F) Anaerobic reduction and reduction kinetic curves of MO. Three biological replicates were performed.

in wastewater treatment. In this study, to synergistically and simultaneously achieve MO degradation and energy harvesting, we constructed a MFC using *S. carassii*-D_5-C_5 as biocatalyst and MO as cathode electrolyte in Fig. 5A. Using MO solution as electron acceptors in cathode (pH = 3, initial MO concentration was 50 mg/L), the MO solution was reduced as the azo-bond broken, becoming clear and transparent gradually. The digital multimeter was used to record the output voltage of the MFCs, as illustrated in Fig. 5B, the MFC inoculated with *S. carassii*-D_5-C_5 only took 3.5 h to quickly increase its bioelectricity generation from the initial 50.0 mV to the maximum voltage of 168.6 mV, while the MFC inoculated with *S. carassii*-D_5 increased from the initial 20.0 mV to 103.0 mV used ~7.5 h at the same condition accompanied with MO degradation. The MFCs inoculated with the engineered strain had smaller internal resistance, suggesting that enhanced riboflavin biosynthesis further strengthened the EET capacity of *S. carassii*-D_5. The power density and polarization curves were calculated and shown in Fig. 5C, which showed that *S. carassii*-D_5-C_5 strain obtained a maximum power density of 192.3 mW/m^2, ~1.6 times higher than that of *S. carassii*-D_5. Notably, the slope of the polarization curve of *S. carassii*-D_5-C_5 was smaller than that of *S. carassii*-D_5, suggesting that the synthesis and secretion of riboflavin reduced the resistance of extracellular electron transfer and thus enhanced the EET [57,58].

Additionally, the biodegrade of MO in MFCs was also investigated. Fig. 5D illustrated that the UV–Vis spectra of MO solution in the cathode of MFCs inoculated with the strain *S. carassii*-D_5-C_5 at different reaction times, the gradual decrease in the absorbance at 465 nm revealed that MO was reduced gradually and suggested that the azo-bond of MO was depleted. The reduction rate of MO by *S. carassii*-D_5-C_5 was further identified by ultraviolet and visible spectrophotometer. As shown in Fig. 5E, *S. carassii*-D_5-C_5 exhibited more efficient degradation of MO. Within approximately 72 h, 86% of MO was reduced by strain *S. carassii*-D_5-C_5, which was 1.3 times higher than that of *S. carassii*-D_5 (66%). To further investigated MO reduction kinetics in MFCs, the pseudo-first-order kinetics equation was used to describe the MO removal kinetics (Eq. (3)). Fig. 5F revealed that the calculated kinetics constant of *S. carassii*-D_5-C_5 was 0.0316 h^{-1}, which was 1.8 times higher than that of *S. carassii*-D_5 (0.0175 h^{-1}). These results suggested that improving the synthesis of riboflavin not only enhanced EET but also promoted MO degradation of *S. carassii*-D_5.

4. Conclusions

In summary, a *Shewanella carassii*-D_5 with strong bioelectricity generation capacity was isolated from activated sludge by the electrochromism of WO_3 nanoclusters, which could reach a maximum power density of 704.6 mW/m^2, ~5.6 times higher than that of the model electroactive strain *S. oneidensis* MR-1 (125.0 mW/m^2). Subsequently, two EET mechanisms of *S. carassii*-D_5 were further identified, based on the analysis of electrophysiological indicators including the amount of *c*-type cytochromes, adhesion biomass, and riboflavin. Notably, these results demonstrated that *S. carassii*-D_5 had a higher density of cytochromes and stronger biofilm formation ability than *S. oneidensis* MR-1, thus facilitating direct EET. Moreover, to enhance the indirect extracellular electron transfer of *S. carassii*-D_5, riboflavin synthesis was further improved from 1.9 to 9.0 mg/g DCW by overexpression of the *ribADEHC* gene cluster from *B. subtili*. The maximum power density of *S. carassii*-D_5-C_5 reached 1286.3 mW/m^2, which was 1.8 times higher than that of *S. carassii*-D_5 (704.6 mW/m^2). For the purpose of promoting the degradation of azo dyes and bioelectricity generation based on the above study, the MFC with *S. carassii*-D_5-C_5 as the anode biocatalyst and MO as the terminal electron acceptor was subsequently constructed. The MO degradation rate of *S. carassii*-D_5-C_5 increased from 66% to 86%, while the maximum power density improved by 1.6 times from 117.9 to 192.3 mW/m^2, respectively. In conclusion, the *S. carassii*-D_5 strain isolated from sludge shows superior organic matter degradation and bioelectricity generation ability, which provides a new possibility for MFCs in pollutant degradation and electricity recovery.

CRediT authorship contribution statement

Chi Yang: contributed equally to the work, Formal analysis, Data curation, Writing – original draft, designed the project, performed experiments, analyzed data, and drafted the manuscript. **Junqi Zhang:** contributed equally to the work, Formal analysis, Data curation, Writing – original draft, designed the project, performed experiments, analyzed data, and drafted the manuscript. **Baocai Zhang:** Formal analysis, Data curation, helped to analyze the experimental data. **Dingyuan Liu:** Formal analysis, Data curation, helped to analyze the experimental data. **Jichao Jia:** Formal analysis, Data curation, helped to analyze the experimental data. **Feng Li:** Supervision, Formal analysis, Data curation, designed and supervised the project, analyzed data, and critically revised the manuscript. **Hao Song:** Supervision, Formal analysis, Data curation, designed and supervised the project, analyzed data, and critically revised the manuscript.

Declaration of competing interest

The authors declare no financial or commercial conflict of interest.

Acknowledgements

This research was supported by the National Key Research and Development Program of China (2018YFA0901300), the National Natural Science Foundation of China (NSFC 32071411, 32001034, and 21621004), Tianjin Science and Technology Plan Project (20JCQNJC00830), and Tianjin Research Innovation Project for Postgraduate Students (2020YJSB045).

Appendix A. Supplementary data

Supplementary data to this article can be found online at https://doi.org/10.1016/j.synbio.2022.04.010.

References

[1] Sun M, Zhai LF, Li WW, Yu HQ. Harvest and utilization of chemical energy in wastes by microbial fuel cells. Chem Soc Rev 2016;45(10):2847–70. https://doi.org/10.1039/c5cs00903k.
[2] Lam KL, Zlatanovic L, van der Hoek JP. Life cycle assessment of nutrient recycling from wastewater: a critical review. Water Res 2020;173:115519. https://doi.org/10.1016/j.watres.2020.115519.
[3] Gude VG. Wastewater treatment in microbial fuel cells–an overview. J Clean Prod 2016;122(20):287–307. https://doi.org/10.1016/j.jclepro.2016.02.022.
[4] Chen H, Simoska O, Lim K, Grattieri M, Yuan M, Dong F, et al. Fundamentals, applications, and future directions of bioelectrocatalysis. Chemial Reviews 2020;120(23):12903–93. https://doi.org/10.1021/acs.chemrev.0c00472.
[5] Do MH, Ngo HH, Guo WS, Liu Y, Chang SW, Nguyen DD, et al. Challenges in the application of microbial fuel cells to wastewater treatment and energy production: a mini review. Sci Total Environ 2018;639(15):910–20. https://doi.org/10.1016/j.scitotenv.2018.05.136.
[6] Moqsud MA, Omine K, Yasufuku N, Hyodo M, Nakata Y. Microbial fuel cell (MFC) for bioelectricity generation from organic wastes. Waste Manag 2013;33(11):2465–9. https://doi.org/10.1016/j.wasman.2013.07.026.
[7] Logan BE, Rossi R, Ragab Aa, Saikaly PE. Electroactive microorganisms in bioelectrochemical systems. Nat Rev Microbiol 2019;17(5):307–19. https://doi.org/10.1038/s41579-019-0173-x.
[8] Chen H, Dong F, Minteer SD. The progress and outlook of bioelectrocatalysis for the production of chemicals, fuels and materials. Nature Catalysis 2020;3(3):225–44. https://doi.org/10.1038/s41929-019-0408-2.
[9] Shi L, Dong H, Reguera G, Beyenal H, Lu A, Liu J, et al. Extracellular electron transfer mechanisms between microorganisms and minerals. Nat Rev Microbiol 2016;14(10):651–62. https://doi.org/10.1038/nrmicro.2016.93.
[10] Peng L, Zhang Y. Cytochrome OmcZ is essential for the current generation by *Geobacter sulfurreducens* under low electrode potential. Electrochim Acta 2017;228:447–52. https://doi.org/10.1016/j.electacta.2017.01.091.
[11] Sun W, Lin Z, Yu Q, Cheng S, Gao H. Promoting extracellular electron transfer of *Shewanella oneidensis* MR-1 by optimizing the periplasmic cytochrome *c* network. Front Microbiol 2021;12. https://doi.org/10.3389/fmicb.2021.727709.
[12] Vellingiri A, Song YE, Munussami G, Kim C, Park C, Jeon B-H, et al. Overexpression of *c*-type cytochrome, CymA in *Shewanella oneidensis* MR-1 for enhanced

bioelectricity generation and cell growth in a microbial fuel cell. J Chem Technol Biotechnol 2019;94(7):2115–22. https://doi.org/10.1002/jctb.5813.
[13] Liu T, Yu YY, Deng XP, Ng CK, Cao B, Wang JY, et al. Enhanced *Shewanella* biofilm promotes bioelectricity generation. Biotechnol Bioeng 2015;112(10):2051–9. https://doi.org/10.1002/bit.25624.
[14] Liu X, Walker DJF, Nonnenmann SS, Sun D, Lovley DR. Direct observation of electrically conductive Pili emanating from *Geobacter sulfurreducens*. mBio 2021;12(4):e0220921. https://doi.org/10.1128/mBio.02209-21.
[15] Liu X, Zhuo S, Jing X, Yuan Y, Rensing C, Zhou S. Flagella act as *Geobacter* biofilm scaffolds to stabilize biofilm and facilitate extracellular electron transfer. Biosens Bioelectron 2019;146:111748. https://doi.org/10.1016/j.bios.2019.111748.
[16] Reguera G, McCarthy KD, Mehta T, Nicoll JS, Tuominen MT, Lovley DR. Extracellular electron transfer via microbial nanowires. Nature 2005;435(7045):1098–101. https://doi.org/10.1038/nature03661.
[17] Martinez CM, Alvarez LH. Application of redox mediators in bioelectrochemical systems. Biotechnol Adv 2018;36(5):1412–23. https://doi.org/10.1016/j.biotechadv.2018.05.005.
[18] Newman DK, Kolter R. A role for excreted quinones in extracellular electron transfer. Nature 2000;405(6782):94–7. https://doi.org/10.1038/35011098.
[19] Marsili E, Baron Daniel B, Shikhare Indraneel D, Coursolle D, Gralnick Jeffrey A, Bond Daniel R. *Shewanella* secretes flavins that mediate extracellular electron transfer. Proc Natl Acad Sci Unit States Am 2008;105(10):3968–73. https://doi.org/10.1073/pnas.0710525105.
[20] Gaffney EM, Minteer SD. A silver assist for microbial fuel cell power. Science 2021;373(6561):1308–9. https://doi.org/10.1126/science.abl3612.
[21] Li F, Li YX, Cao YX, Wang L, Liu CG, Shi L, et al. Modular engineering to increase intracellular NAD(H/(+)) promotes rate of extracellular electron transfer of *Shewanella oneidensis*. Nat Commun 2018;9(1):3637. https://doi.org/10.1038/s41467-018-05995-8.
[22] Zhang J, Chen Z, Liu C, Li J, An X, Wu D, et al. Construction of an acetate metabolic pathway to enhance electron generation of engineered *Shewanella oneidensis*. Front Bioeng Biotechnol 2021;9(1007). https://doi.org/10.3389/fbioe.2021.757953.
[23] Li F, Li Y, Sun L, Chen X, An X, Yin C, et al. Modular engineering intracellular NADH regeneration boosts extracellular electron transfer of *Shewanella oneidensis* MR-1. ACS Synth Biol 2018;7(3):885–95. https://doi.org/10.1021/acssynbio.7b00390.
[24] Li F, Wang L, Liu C, Wu D, Song H. Engineering exoelectrogens by synthetic biology strategies. Current Opinion in Electrochemistry 2018;10:37–45. https://doi.org/10.1016/j.coelec.2018.03.030.
[25] Joicy A, Song YC, Lee CY. Electroactive microorganisms enriched from activated sludge remove nitrogen in bioelectrochemical reactor. J Environ Manag 2019;233(1):249–57. https://doi.org/10.1016/j.jenvman.2018.12.037.
[26] Doyle LE, Yung PY, Mitra SD, Wuertz S, Williams RBH, Lauro FM, et al. Electrochemical and genomic analysis of novel electroactive isolates obtained via potentiostatic enrichment from tropical sediment. J Power Sources 2017;356(15):539–48. https://doi.org/10.1016/j.jpowsour.2017.03.147.
[27] Adhikari S, Swain R, Sarkar D, Madras G. Wedge-like WO_3 architectures for efficient electrochromism and photoelectrocatalytic activity towards water pollutants. Mol Catal 2017;432:76–87. https://doi.org/10.1016/j.mcat.2017.02.009.
[28] He H, Yuan S-J, Tong Z-H, Huang Y-X, Lin Z-Q, Yu H-Q. Characterization of a new electrochemically active bacterium, *Lysinibacillus sphaericus* D-8, isolated with a WO_3 nanocluster probe. Process Biochem 2014;49(2):290–4. https://doi.org/10.1016/j.procbio.2013.11.008.
[29] Yang Z-C, Cheng Y-Y, Zhang F, Li B-B, Mu Y, Li W-W, et al. Rapid detection and enumeration of exoelectrogenic bacteria in lake sediments and a wastewater treatment plant using a coupled wo_3 nanoclusters and most probable number method. Environ Sci Technol Lett 2016;3(4):133–7. https://doi.org/10.1021/acs.estlett.6b00112.
[30] Marques AC, Santos L, Costa MN, Dantas JM, Duarte P, Goncalves A, et al. Office paper platform for bioelectrochromic detection of electrochemically active bacteria using tungsten trioxide nanoprobes. Sci Rep 2015;5:9910. https://doi.org/10.1038/srep09910.
[31] Zhou S, Wen J, Chen J, Lu Q. Rapid measurement of microbial extracellular respiration ability using a high-throughput colorimetric assay. Environ Sci Technol Lett 2015;2(2):26–30. https://doi.org/10.1021/ez500405t.
[32] Wen J, Zhou S, Chen J. Colorimetric detection of *Shewanella oneidensis* based on immunomagnetic capture and bacterial intrinsic peroxidase activity. Sci Rep 2014;4:5191. https://doi.org/10.1038/srep05191.
[33] Huang T, Liu L, Tao J, Zhou L, Zhang S. Microbial fuel cells coupling with the three-dimensional electro-Fenton technique enhances the degradation of methyl orange in the wastewater. Environ Sci Pollut Control Ser 2018;25(18):17989–8000. https://doi.org/10.1007/s11356-018-1976-4.
[34] Xu M, Guo J, Cen Y, Zhong X, Cao W, Sun G. *Shewanella decolorationis* sp. nov., a dye-decolorizing bacterium isolated from activated sludge of a waste-water treatment plant. Int J Syst Evol Microbiol 2005;55(Pt 1):363–8. https://doi.org/10.1099/ijs.0.63157-0.
[35] Liu F, Xu M, Chen X, Yang Y, Wang H, Sun G. Novel strategy for tracking the microbial degradation of azo dyes with different polarities in living cells. Environ Sci Technol 2015;49(19):11356–62. https://doi.org/10.1021/acs.est.5b02003.
[36] Xiao X, Liu QY, Li TT, Zhang F, Li WW, Zhou XT, et al. A high-throughput dye-reducing photometric assay for evaluating microbial exoelectrogenic ability. Bioresour Technol 2017;241:743–9. https://doi.org/10.1016/j.biortech.2017.06.013.
[37] Fang Z, Song HL, Cang N, Li XN. Electricity production from Azo dye wastewater using a microbial fuel cell coupled constructed wetland operating under different operating conditions. Biosens Bioelectron 2015;68(15):135–41. https://doi.org/10.1016/j.bios.2014.12.047.
[38] Cheng L, Min D, He RL, Cheng ZH, Liu DF, Yu HQ. Developing a base-editing system to expand the carbon source utilization spectra of *Shewanella oneidensis* MR-1 for enhanced pollutant degradation. Biotechnol Bioeng 2020;117(8):2389–400. https://doi.org/10.1002/bit.27368.
[39] Feng Y, Yang L, Liu J, Logan BE. Electrochemical technologies for wastewater treatment and resource reclamation. Environ Sci : Water Research & Technology 2016;2(5):800–31. https://doi.org/10.1039/c5ew00289c.
[40] Lin T, Ding W, Sun L, Wang L, Liu C-G, Song H. Engineered *Shewanella oneidensis*-reduced graphene oxide biohybrid with enhanced biosynthesis and transport of flavins enabled a highest bioelectricity output in microbial fuel cells. Nano Energy 2018;50:639–48. https://doi.org/10.1016/j.nanoen.2018.05.072.
[41] Feng J, Qian Y, Wang Z, Wang X, Xu S, Chen K, et al. Enhancing the performance of Escherichia coli-inoculated microbial fuel cells by introduction of the phenazine-1-carboxylic acid pathway. J Biotechnol 2018;275:1–6. https://doi.org/10.1016/j.jbiotec.2018.03.017.
[42] Yuan SJ, Li WW, Cheng YY, He H, Chen JJ, Tong ZH, et al. A plate-based electrochromic approach for the high-throughput detection of electrochemically active bacteria. Nat Protoc 2014;9(1):112–9. https://doi.org/10.1038/nprot.2013.173.
[43] Myers Charles R, Nealson Kenneth H. Bacterial manganese reduction and growth with manganese oxide as the sole electron acceptor. Science 1988;240(4857):1319–21. https://doi.org/10.1126/science.240.4857.1319.
[44] Zhou L, Deng D, Zhang Y, Zhou W, Jiang Y, Liu Y. Isolation of a facultative anaerobic exoelectrogenic strain LZ-1 and probing electron transfer mechanism in situ by linking UV/Vis spectroscopy and electrochemistry. Biosens Bioelectron 2017;90:264–8. https://doi.org/10.1016/j.bios.2016.11.059.
[45] Frobose NJ, Bjedov S, Schuler F, Kahl BC, Kampmeier S, Schaumburg F. Gram staining: a comparison of two automated systems and manual staining. J Clin Microbiol 2020;58(12). https://doi.org/10.1128/JCM.01914-20.
[46] Yang Y, Ding Y, Hu Y, Cao B, Rice SA, Kjelleberg S, et al. Enhancing bidirectional electron transfer of *Shewanella oneidensis* by a synthetic flavin pathway. ACS Synth Biol 2015;4(7):815–23. https://doi.org/10.1021/sb500331x.
[47] Han H-X, Shi C, Yuan L, Sheng G-P. Enhancement of methyl orange degradation and power generation in a photoelectrocatalytic microbial fuel cell. Appl Energy 2017;204:382–9. https://doi.org/10.1016/j.apenergy.2017.07.032.
[48] Coursolle D, Baron DB, Bond DR, Gralnick JA. The Mtr respiratory pathway is essential for reducing flavins and electrodes in *Shewanella oneidensis*. J Bacteriol 2010;192(2):467–74. https://doi.org/10.1128/JB.00925-09.
[49] Cao Y, Song M, Li F, Li C, Lin X, Chen Y, et al. A synthetic plasmid toolkit for *Shewanella oneidensis* MR-1. Front Microbiol 2019;10:410. https://doi.org/10.3389/fmicb.2019.00410.
[50] Xiao Y, Zhang E, Zhang J, Dai Y, Yang Z, Christensen HEM, et al. Extracellular polymeric substances are transient media for microbial extracellular electron transfer. Sci Adv 2017;3(7):e1700623. https://doi.org/10.1126/sciadv.1700623.
[51] Okamoto A, Hashimoto K, Nealson KH, Nakamura R. Rate enhancement of bacterial extracellular electron transport involves bound flavin semiquinones. Proc Natl Acad Sci Unit States Am 2013;110(19):7856–61. https://doi.org/10.1073/pnas.1220823110.
[52] Zhu J, Wang M, Zhang H, Yang S, Song KY, Yin R, et al. Effects of hydrophilicity, adhesion work, and fluid flow on biofilm formation of PDMS in microfluidic systems. ACS Appl Bio Mater 2020;3(12):8386–94. https://doi.org/10.1021/acsabm.0c00660.
[53] Goswami P, Singh HD. Different modes of hydrocarbon uptake by two *Pseudomonas* species. Biotechnol Bioeng 1991;37(1):1–11. https://doi.org/10.1002/bit.260370103.
[54] Light SH, Su L, Rivera-Lugo R, Cornejo JA, Louie A, Iavarone AT, et al. A flavin-based extracellular electron transfer mechanism in diverse Gram-positive bacteria. Nature 2018;562(7725):140–4. https://doi.org/10.1038/s41586-018-0498-z.
[55] Cai P-J, Xiao X, He Y-R, Li W-W, Chu J, Wu C, et al. Anaerobic biodecolorization mechanism of methyl orange by *Shewanella oneidensis* MR-1. Appl Microbiol Biotechnol 2012;93(4):1769–76. https://doi.org/10.1007/s00253-011-3508-8.
[56] Huang L, Tang J, Chen M, Liu X, Zhou S. Two modes of riboflavin-mediated extracellular electron transfer in *Geobacter uraniireducens*. Front Microbiol 2018;9:2886. https://doi.org/10.3389/fmicb.2018.02886.
[57] Zhang ZB, Cheng ZH, Wu JH, Yue ZB, Wang J, Liu DF. Engineering of salt-tolerant *Shewanella aquimarina* XMS-1 for enhanced pollutants transformation and electricity generation. Sci Total Environ 2022;807(Pt 3):151009. https://doi.org/10.1016/j.scitotenv.2021.151009.
[58] Edel M, Sturm G, Sturm-Richter K, Wagner M, Ducassou JN, Coute Y, et al. Extracellular riboflavin induces anaerobic biofilm formation in *Shewanella oneidensis*. Biotechnol Biofuels 2021;14(1):130. https://doi.org/10.1186/s13068-021-01981-3.